JOURNAL OF CATALYSIS 148, 779–786 (1994)

A Probe of Brønsted Site Acidity in Zeolites: ^{13}C Chemical Shift of Acetone

A. I. Biaglow,* R. J. Gorte,* G. T. Kokotailo,* and David White†

*Department of Chemical Engineering, University of Pennsylvania, Philadelphia, Pennsylvania 19104; and †Department of Chemistry, University of Pennsylvania, Philadelphia, Pennsylvania 19104

Received February 22, 1994; revised April 20, 1994

^{13}C NMR spectroscopy has been used to characterize the adsorption of acetone (C-2 ^{13}C-labeled 2-propanone), at coverages of less than one molecule per Brønsted-acid site, in the molecular sieves H–ZSM-5, H–mordenite, H–ZSM-12, H–ZSM-22, chemically dealuminated H–Y, SAPO-5, MgAPO-5, and BeAPO-5. It is shown that the trace of the chemical shift tensor for the carbonyl carbon at 125 K measures the ability of the site to form a hydrogen bond with the carbonyl oxygen and, therefore, can be used as a measure of the intrinsic acidity of the site. The sites in all of the materials investigated were nearly homogeneous, with the isotropic shifts for most of the molecular sieves falling in the range observed for solutions of acetone in trifluoroacetic acid. In addition, the lineshape and linewidths of the ^{13}C NMR powder patterns at room temperature provide a measure of the molecular motion of adsorbed acetone and are strongly affected by the size of the framework channels.

INTRODUCTION

It is well recognized that the primary process in many acid-catalyzed reactions involving zeolites requires the transfer of a proton from the Brønsted-acid site on the zeolite to the chemisorbed molecule, or at least the formation of a hydrogen-bonded complex (1). Although reactions depend on many additional factors relating to the interactions of the adsorbed species with the zeolite cavities and to the local and extended dynamics of the adsorbed molecules (2, 3), the extent to which proton transfer or hydrogen bonding occurs between the Brønsted-acid site and the adsorbate is extremely important for understanding differences observed between various materials and for developing a detailed understanding of reactions in zeolites.

There are many techniques for evaluating the strengths of acid sites in zeolites using both macroscopic and microscopic probes, including calorimetric measurements of simple probe molecules (4), measurements of catalytic activity and product distributions (5), spectroscopic measurements (6), and other methods (7). It is not the purpose of this paper to evaluate these techniques or discuss the specific information they provide. Of interest here is the primary process on adsorption of a molecule associated with the changes in electronic structure resulting from the interactions with the acid site, a process which is masked or not observed in many other techniques. Such changes are analogous to solvent effects which have been extensively studied using ^{13}C chemical shifts of probe molecules in solution (8) and which we now employ in the study of molecular sieves.

In a recent note, we reported results from a ^{13}C NMR study of acetone adsorption in H–ZSM-5 that suggested the possibility that this molecule could be used as a probe of the Brønsted-acid site environment (9), particularly at low surface coverages, below one molecule per acid site. At such coverages, the adsorbed molecules appear to be localized at the sites at room temperature, at least within the time scale of the NMR experiment, so that averaging of the chemical shift due to exchange, either with other Brønsted-acid sites or with other sites in the zeolite, is minimal. Second, there is a large isotropic chemical shift of the carbonyl carbon relative to the neat solid associated in large part with the formation of a hydrogen bond between the carbonyl oxygen and the zeolite proton. The presence of weaker interactions between other atoms of the adsorbed molecule and the zeolite also plays a role; however, their main effect is in restricting molecular reorientations and translations reflected in changes in the line shape with temperature. Finally, the acetone molecule, despite changes in electronic structure at the Brønsted-acid sites, does not undergo measurable reaction at room temperature and low surface coverage, simplifying interpretation of the spectroscopic data.

The sensitivity of the isotropic chemical shift of the carbonyl carbon of acetone to different solvent environments has been clearly demonstrated in the comprehensive studies by Maciel and collaborators (8). They show that, in moderately acidic solvents such as formic acid or trifluoroacetic acid, these shifts are related to the varying tendency of such solvents to form hydrogen bonds. The

0021-9517/94 $6.00

valence bond description of this tendency to form hydrogen bonds in solution is represented by a superposition of several resonance structures, but *not* by any exchange processes involving chemical equilibria. The range of isotropic chemical shifts is large, varying from 3.7 ppm in methanol to 14.1 ppm in trifluoroacetic acid, relative to pure liquid acetone, and is entirely due to the changes in charge density in the acetone molecule induced by this tendency to form hydrogen bonds. This is clearly an *environmental* effect. Given that the magnitude of the isotropic shift in zeolites (9, 35) (relative to the pure liquid) is comparable to that in the weak acids, it should be possible, in a similar manner, to determine the varying tendencies to form hydrogen bonds in different zeolites at Brønsted sites and, in the absence of site exchange, the site distribution or the number of different types of sites. Just as in the case of moderately acidic solvents, such a classification of zeolites based on ^{13}C carbonyl shifts should provide a scale for determining the intrinsic ability of a Brønsted site to transfer protons in the formation of hydrogen bonds and is therefore a measure of acidity. This measure is not a thermodynamic equilibrium constant but a *microscopic* measure relating to the average strength or length of the hydrogen bond. Admittedly, from a microscopic view, the situation in liquid solutions is different from that in solid acids. In the former case, the measured chemical shifts represent time averages of the fluctuations in the solvent environment. In the latter case, if the acetone molecule is localized, the shifts represent spatial or site averages. These averages are nevertheless directly related when the diffusion in the solvent is rapid. It should be noted that in solid acids, unlike liquid solutions, it is possible to measure the components of the shielding tensor by NMR studies of the adsorbed molecule in a "rigid-lattice" regime. This, in principle, can provide more detailed information concerning the changes in electronic structure of the chemisorbed species due to the local environment at the acid site (10).

In this paper, we report the ^{13}C NMR results from acetone adsorption in H–ZSM-5, H–ZSM-12, H–ZSM-22, H–mordenite, chemically dealuminated H–Y, H–[Ga]ZSM-5, MgAPO-5, BeAPO-5, and SAPO-5. These materials were chosen in order to examine the effect of both structure and composition on acidity. H–ZSM-5 consists of interconnecting, 10-membered rings. H–ZSM-12 and H–mordenite contain one-dimensional, 12-membered-ring channels, with 8-membered rings connecting the channels in mordenite. H–ZSM-22 consists of one-dimensional, 10-membered-ring channels and is unusual among zeolites in that it does not contain any 4-membered rings. H–[Ga]ZSM-5 has the ZSM-5 structure but the lattice charge is due to the Ga^{+3} ions rather than Al^{+3}. SAPO-5 consists of one-dimensional, 12-membered-ring channels, but the basic building blocks are alternating AlO_4 and PO_4 tetrahedra, with acidity introduced by the substitution of SiO_4 for PO_4. MgAPO-5 and BeAPO-5 have the same structure as SAPO-5, with Brønsted acidity introduced by the incorporation of Mg^{+2} or Be^{+2} for Al^{+3}, respectively.

EXPERIMENTAL

Molecular Sieves

The molecular sieves used in this study are listed in Table 1, along with some of their important properties. Two H–ZSM-5 samples were investigated in order to determine the effect of synthesis procedure. H–ZSM-5A was the same sample as that used in Ref. (9) and was prepared using hydrothermal conditions and TPA–Br (Alfa/Morton Thiokol, Inc.) as a template. H–ZSM-5B was obtained from Alcoa and had been prepared without a template. H-ZSM-12 was also prepared under hydrothermal conditions described in an earlier publication (11). The mordenite sample was obtained in the ammonium-ion form from Conteka and had been steamed and acid leached to a bulk Si/Al ratio of 15. The H–ZSM-22 sample was synthesized hydrothermally using published procedures (12). The synthesis and characterization of H–[Ga]ZSM-5, SAPO-5, and MgAPO-5 samples have also been reported (13–15). The H–[Ga]ZSM-5 sample

TABLE 1

Physical Characteristics of the Molecular Sieves

Sample	[Al] (μmol/g)	[H⁺] (μmol/g)	Crystallographic channel dimensions[c] (Å)
H–ZSM-5	430	366	8.4 × 7.7, elliptical, straight 8.1 × 7.7, elliptical, sinusoidal
H–ZSM-5B	620	600	same as H–ZSM-5A
H–ZSM-12	—	155	9.5 × 8.3, elliptical, straight
H–ZSM-22	460	345	8.2 × 7.6, elliptical, straight[d]
H–[Ga]ZSM-5	430[a,b]	406	same as H–ZSM-5A
H-Mordenite	1180	700	10.6 × 9.2, elliptical, straight 7.5 × 6.4, elliptical, sinusoidal
H–Y	2520	700	
SAPO-5	2790[a,b]	230	10.0, circular, straight
BeAPO-5	160[a,b]	80	same as SAPO-5
MgAPO-5	160[a,b]	100	same as SAPO-5

[a] Measured from the gel for the as-synthesized materials.

[b] μmol/g of Ga for the H–[Ga]ZSM-5, Si for the SAPO-5, Be for the BeAPO-5, and Mg for the MgAPO-5.

[c] Point-to-point distances between coplanar O atoms on opposite ends of the channel.

[d] The 10-membered ring defining this channel is nonplanar. The 8.2-Å dimension is a projection onto a plane which is perpendicular to the axis of the channel.

had a Si/Ga_2 ratio of 75, while the SAPO-5 sample was 17 mol% Si (i.e., Si/(Si + P + A) = 0.17), based on the concentrations in the gel.

The chemically dealuminated H–Y sample was prepared by a double dealumination of an ammonium ion-exchanged Na–Y, using ammonium hexafluorosilicate and procedures outlined in the literature (16, 17). In the first step of dealumination, 3.00 g of an ion-exchanged, Y zeolite with an Si/Al ratio of 2.5 was added to 200.00 g of a solution containing 12.20 g of ammonium acetate in deionized water. While this mixture was being heated in a vessel at 350 K, 2.00 g of a solution containing 0.90 g of ammonium hexafluorosilicate in 25.00 g of ammonium acetate was added dropwise. This mixture was stirred at 350 K for 3 h, filtered, and then dried in an oven at 470 K for 20 min. Following a second ammonium-ion exchange with an ammonium sulfate solution, a second dealumination step was performed which was identical to the first except that the starting weight of the zeolite was 1.00 g and the other ingredients were scaled back proportionally. The bulk Al content for this sample, 29 Al/unit cell, agreed very well with the framework Al content calculated from the XRD lattice parameter (16), showing that this material contained very little nonframework Al.

Each of the materials was characterized by X-ray diffraction and was highly crystalline, with no additional phases. Bulk concentrations were measured using atomic absorption spectroscopy and Brønsted-acid site concentrations were determined from simultaneous temperature-programmed-desorption (TPD) and thermogravimetric-analysis (TGA) measurements with isopropylamine. The TPD–TGA technique relies on the fact that isopropylamine molecules adsorbed at Brønsted-acid sites decompose to propene and ammonia between 575 and 650 K during desorption (18). On high-silica zeolites, like H–ZSM-5, H–ZSM-12, and H–mordenite, the site concentrations determined in this manner are close to one per framework Al (19), with the differences being associated with the presence of small amounts of nonframework Al. Similarly, site concentrations for Mg- and Be-substituted AlPO-5 are very close to the Mg and Be content, respectively (15). The site concentrations are not simply equal to the framework Al content in the H–Y sample (20) or the Si content in SAPO-5 (14). In H–Y, it was demonstrated that only a fraction of the hydroxyls, those associated with the high-frequency IR band at 3640 cm^{-1}, form strong Brønsted-acid sites which are capable of decomposing the amine molecule in TPD–TGA (17, 20). In SAPO-5, only those hydroxyls associated with isolated Si atoms lead to strong Brønsted-acid sites (14). However, these materials do have well-defined Brønsted-acid sites and the site concentrations are not a function of the probe molecule used in the measurement (14, 20, 21).

Acetone-Doped NMR Samples

In previous studies (9, 22), it was demonstrated that in order to probe the local environment of the Brønsted site uncomplicated by exchange of chemisorbed or physisorbed species and bimolecular reactions, it was necessary to dose the molecular sieves with acetone at surface coverages that were less than one molecule per Brønsted site. This necessitated the use of ^{13}C enrichment (99% carbonyl-labeled, Cambridge Isotope Laboratories, Inc.) in order to reduce the acquisition time of the NMR spectra.

The samples, ranging in size from 150 to 300 mg, were initially degassed and weighed in a Cahn microbalance at a pressure of 10^{-6} Torr and 700 K. The samples were then introduced into a specially designed vacuum system in which the materials could be spread into a bed 0.5 mm thick or less, where they were degassed at 700 K to 10^{-6} Torr. The samples were then exposed to controlled amounts of C2, 99%-enriched [^{13}C]acetone from a calibrated system that permitted the adsorbate coverage to be known to within ±1–2%, equilibrated, and sealed in glass sample tubes without exposure to air. From the examination of a large number of samples prepared in different ways and exposed for different times, it was found that shallow-bed adsorption leads to rapid and reproducible equilibration. The diameter and length of the sealed sample tubes were such as to permit direct insertion in a static, double-resonance NMR probe. For the magic-angle spinning experiments (MAS), a portion of the sample, removed from the sealed sample tubes in an inert nitrogen environment, was introduced to O-ring-sealed rotors of a Doty MAS probe (DSI-574). No measurable changes in frequencies or lineshape occurred upon transfer of the samples from the vacuum-sealed glass containers to the O-ringed-sealed Doty rotors in a nitrogen environment for MAS experiments. The moles of adsorbed acetone in all samples were also determined from the intensities of the free induction decay (FID) by comparison with standard ^{13}C samples. The results in all cases were in good agreement with the measured surface coverages. The acetone coverages for each sample are reported in units of molecules per Brønsted site and are given in Table 2.

The ^{13}C NMR spectra were obtained at a field of 3.5 T using a home-built spectrometer previously described (23). The line frequencies and shapes were determined from the observation of both proton-decoupled FIDs and Hahn echoes, with and without MAS. The echo sequence consisted of a series of $90°–\tau–180°–\tau$ pulses in quadrature with a delay time, τ, of 30 μs. Room-temperature and low-temperature rigid-lattice regime, MAS experiments were performed to establish the isotropic chemical shifts

TABLE 2

Trace[a] of the Chemical Shift Tensor of the C-2 Carbon of Chemisorbed Acetone at 125 K Relative to the Neat Solid

Sample	Surface coverage (molecules/H^+)	Primary site shift[b] at 125 K (ppm)	Secondary site shift[b] and % abundance (ppm)	(%)	Method[d]
H–ZSM-5A	0.85	16.9	26.6	(1)	HE
H–ZSM-5B	0.85	16.8	—	(<1)[c]	HE
H–ZSM-12	0.70	16.7	—	(<1)[c]	HE
H–ZSM-22	0.80	18.7	—	(<1)[c]	HE
H–[Ga]ZSM-5	0.78	16.1	—	(<1)[c]	HE
H–mordenite	0.80	15.1	26.8	(10)	HE
H–Y	0.74	12.9	25.7	(2)	HE
SAPO-5	0.66	10.1	25.6	(2)	CP
BeAPO-5	0.92	16.7	23.2	(5)	CP
MgAPO-5	0.90	17.7	23.6	(10)	CP

[a] The trace, in general, corresponds very closely to the isotropic chemical shift.
[b] Uncertainty is ±0.4 ppm.
[c] Not observable within the signal to noise level.
[d] HE, Hahn echo; CP; cross polarization.

of the chemisorbed acetone. At room temperature, the Doty probe had a maximum spinning frequency of approximately 4 kHz and 2 kHz at temperatures as low as 120 K. Because of possible spectral distortions, ^1H–^{13}C cross-polarization signal enhancement was used only in the room-temperature measurements of the proton-decoupled static ^{13}C linewidths of the aluminophosphates, where the ^{13}C spin count is very low. This is especially important when multiple sites of different intensities are present. In all other cases, the integrated intensities reflect the abundances for our choice of repetition rates, which take into account spin–lattice relaxation. The total spin count, even at low temperatures, was always consistent with the initial spin count so that all spectral features are displayed in the Fourier transforms of the FIDs or Hahn echoes.

RESULTS

The experimental results focus on two characteristics of chemisorbed acetone molecules at the Brønsted sites in a variety of environments provided by the different molecular sieves. The first, the isotropic chemical shift (trace of the shielding tensor), determines the number of different adsorption sites and their corresponding environments. The second, the powder lineshape of a partially motionally averaged chemical shift tensor of the ^{13}C carbonyl atom, relates to the anisotropy of the molecular motions in the vicinity of the Brønsted site. Although the trace of the shielding tensors appeared to be independent of temperature within experimental error (±0.4 ppm), the values reported here are for the rigid lattice, so that dynamical effects need not be considered. Nevertheless it is worth noting that molecular motion, which does not include exchange with physisorbed species at these low surface coverages, does not appreciably affect the isotropic shifts, a good indication of localization of the chemisorbed acetone.

In Fig. 1, typical proton-decoupled MAS spectra are shown for the case of the H–[Ga]ZSM-5 at two different spinning speeds. The frequency of the zero-order sideband of the inhomogeneously broadened spin system, which does not change for different MAS speeds, corresponds to the trace of the anisotropic chemical shift tensor. The linewidth of the zero-order side band at the lowest temperature, 125 K, when corrected for field inhomogeneity and bulk susceptibility effects, is less than 2 ppm and is typical of all the samples examined. Such narrow lines are indicative not only of site uniformity (or lack of a site distribution) but also of long correlation times for rotational reorientations in a very slow motion regime. Further line narrowing of the zero-order sideband with decreasing temperature is probably small and would only occur as a result of coherent spatial averaging on MAS in the strong-collision limit (24).

A summary of the data for all of the zeolite and aluminophosphate samples is given in Table 2. The shifts are given in ppm relative to that observed for the neat solid at 125 K in the same NMR probe. The shifts are all downfield relative to those of the neat solid as well as TMS. While most of the samples gave evidence for only a single site, additional peaks were observed in the NMR spectra for a few of the samples. The downfield shifts for these secondary sites relative to the neat solid (~25 ppm), together

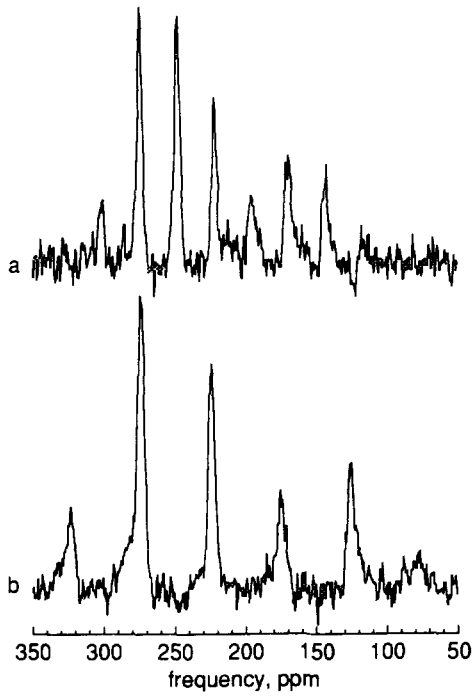

FIG. 1. Proton-decoupled, magic angle spinning spectra of ^{13}C carbonyl of acetone chemisorbed on H–[Ga]ZSM-5 at 125 K and surface coverage of 0.78 acetone molecules per Brønsted site Two hundred fifty-six scans with a repetition time of 30 s were taken. Spinning speed was (a) 0.94 kHz, (b) 1.87 kHz.

with estimated abundances (in brackets), are also given in Table 2. In the case of the SAPO-5, BeAPO-5, and MgAPO-5, the intensity of the NMR signal due to the secondary site relative to that of the primary site may be artificially amplified due to the necessity of using cross polarization for signal enhancement. In experiments using a steamed H–Y sample containing significant amounts of nonframework Al, which will be reported in a separate publication (25), acetone was present at the secondary sites in significant quantities. It seems likely, therefore, that the presence of small amounts of a second type of site are related to nonframework species.

In Fig. 2 we demonstrate powder pattern linewidth and lineshape differences at room temperature for two zeolites, H-ZSM-5A and H–Y, obtained in the static NMR probe under conditions of proton decoupling. In general, the lineshapes are characteristic of the partially motionally averaged, C-2 ^{13}C chemical shift tensor broadened by heteronuclear ^{27}Al–^{13}C dipolar interactions. Based on a second-moment calculation (26) for Al–C distances, 4 to 5 Å, this is estimated to fall in the range 6–13 ppm in the zeolites and perhaps as much as twice that in the BeAPO-5 and MgAPO-5. A summary of the linewidths for each of the molecular sieves is given in Table 3 together with the largest and smallest van der Waals cross section of the channels in the different sieves.

Although it is not the purpose of this paper to discuss the elements of the chemical shift tensor of chemisorbed acetone, the rigid-lattice, or low-temperature, results for H–[Al]ZSM-5 are nevertheless shown in Fig. 2 for two reasons. The first is to note that, with the possible exception of H–ZSM-22, all the materials show an incomplete evolution of a non-axially symmetric powder pattern of the chemical shift anisotropy at room temperature. Although we have yet to achieve the necessary precision to describe the dynamics of this evolution with temperature, we have been able to show that the lineshape does not measurably change below approximately 150 K in all cases. In all probability, the spectrum at this temperature represents the anisotropy of the rigid lattice. Second, we had earlier reported the principal elements of the chemical shielding tensor determined from data taken at room temperature for H–ZSM-5 (9) under the assumption that these data represented the rigid lattice. Based on the present

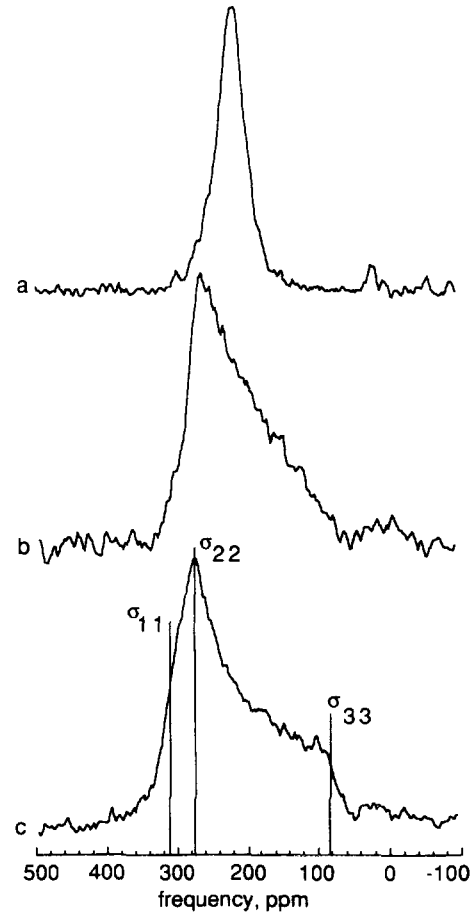

FIG. 2. Proton-decoupled powder patterns of ^{13}C carbonyl of chemisorbed acetone. (a) H–Y at 295 K and 0.74 acetone molecules per Brønsted site; 20,200 scans, repetition time, 5 s; (b) H–ZSM-5 at 295 K and 0.85 acetone molecules per Brønsted site; 18,320 scans, repetition time, 2 s; (c) H–ZSM-5 at 125 K and 0.85 acetone molecules per Brønsted site; 6144 scans, repetition time, 30 s.

TABLE 3

Chemical Shift Powder Linewidths of the [^{13}C]Carbonyl Carbon of Chemisorbed Acetone at 295 K

Sample	Surface coverage (molecules/H$^+$)	Linewidth of primary Brønsted site at 295 K (ppm)	Largest and smallest van der Waals channel cross, section[c] (Å)
H-ZSM-22	0.80	230 ± 8[a]	5.4 × 4.8
H-ZSM-5A	0.85	200 ± 8[a]	5.6 × 4.9
H-ZSM-5B	0.85	200 ± 8[a]	5.6 × 4.9
H-[Ga]ZSM-5	0.78	200 ± 8[a]	5.6 × 4.9
H-ZSM-12	0.70	103 ± 5[b]	6.2 × 5.5
H-mordenite	0.80	103 ± 8[b]	7.8 × 6.4
SAPO-5	0.66	88 ± 10[b]	7.2 (cylindrical)
MgAPO-5	0.90	84 ± 10[b]	7.3 (cylindrical)
H-Y	0.74	46 ± 4[b]	7.2 × 13.4

[a] $\sigma_{11}-\sigma_{33}$ of partially or fully developed "rigid-lattice" non-axially symmetric powder pattern.

[b] Full width at half-maximum of a combination Lorentzian and Gaussian lineshape centered at the isotropic shift.

[c] Calculated using the channel dimensions in Table 1 and the van der Waals radius of oxygen of 1.4 Å.

results, this is clearly not the case. The corrected rigid-lattice values determined from the low-temperature data shown in Fig. 2 are $\sigma_{11} = 312 \pm 5$, $\sigma_{22} = 276 \pm 5$, and $\sigma_{33} = 82 \pm 7$ ppm relative to TMS. The trace of the tensor, $\bar{\sigma} = 223.2 \pm 2$, is within 1 ppm of the value obtain in the low-temperature MAS experiment. These components are more in line with ^{13}C carbonyl shielding tensors for the large number of molecules reported in the literature (27). It is found that the most shielded component, σ_{33}, is not very sensitive to the molecular environment of the carbonyl group and that downfield changes relative to the pure solid, particularly in σ_{22}, are strongly affected by hydrogen bonding (28). Calculations are presently underway to explore the effect of hydrogen bonding on the shielding tensor and the associated change in the electronic structure of the chemisorbed acetone. This will be reported separately at a later date (29).

Two types of lineshapes corresponding to a partially motionally averaged anisotropy of the chemical shift were observed in the experiments involving the static probe. The narrower lines were centered about the trace of the shielding tensor and could be fitted to a combination of Lorentzian and Gaussian lineshapes. The broader powder patterns are asymmetric but smaller in width than those in the non-axially symmetric chemical shift tensor of the rigid lattice. The linewidths given in these cases are $(\sigma_{11}-\sigma_{33})$ of an unbroadened tensor that best fit the data. In the case of H-ZSM-22, no measurable change in lineshape could be detected upon cooling the sample to 125 K, suggestive of a fully developed anisotropic powder pattern. Unfortunately, the signal to noise was not sufficiently large to permit the observation of significant differences between this zeolite and H-[Al]ZSM-5 discussed above.

DISCUSSION

The NMR data reported here provide interesting insights concerning the Brønsted-acid sites in zeolites and other molecular sieves. Because the chemisorbed acetone molecules appear to be localized at low surface coverages, at least on the NMR time scale (10^{-2} to 10^{-3} s), the spectra are indicative of the chemical environment of the acid site unaffected by bimolecular processes which can frequently dominate reaction rates and other measures of acidity. To a first approximation, the measured chemical shifts relative to that of neat solid acetone are indicative of an intrinsic acidity for each of the materials. The shifts are intimately connected to the change in the electronic structure on adsorption, in particular the charge distribution in the vicinity of the [^{13}C]carbonyl carbon. On the other hand, the anisotropic lineshapes, modulated by the localized molecular reorientations at the Brønsted site, provide insight into the magnitude and angular anisotropy of the barriers to rotation in the channels of the molecular sieves.

It has already been demonstrated by Maciel and Natterstad that the isotropic chemical shifts of acetone in moderately acidic media are the result of hydrogen bonding with the carbonyl carbon (8). For example, in the series of acids formic acid, dichloroacetic acid, and trifluoroacetic acid, the chemical shifts are 9.1, 11.9, and 14.1 ppm, respectively. If one uses this scale as a measure of Brønsted-acid site strengths in molecular sieves, one finds that the environments of all of the materials we examined here, with the exception of SAPO-5 and H-Y, are comparable to that in trifluoroacetic acid. In the latter cases, the environments correspond to somewhat weaker acids. The assumption here is that the isotropic chemical shifts of the probe molecule acetone in solid acids scale with environment in a manner identical to that of solutions. This assumption does not contradict statements in a recent paper that heats of adsorption for amines in H-ZSM-5 scale with gas-phase proton affinities (30). The amines are strong bases and can be shown, spectroscopically, to be protonated in the zeolite (31). Therefore, the energetics is dominated by the reaction to form the protonated species at the acid site environment and thus scales with proton affinity (30). In weak bases such as acetone the dominant species is unprotonated so that one measures effects associated with the modification of the charge distribution by the acid site environment.

Two additional conclusions can be reached based on the ^{13}C chemical shift results. First, the acid sites must be relatively homogeneous in each of the materials, the

linewidth of the zero-order sideband in the MAS spectrum at low temperatures being less than 2 ppm in all of the materials. Second, the range of chemical shifts in both the zeolite and the aluminophosphate structures is not large; however, the differences between materials are significant and reproducible. Since the acid sites in all of the materials are relatively dilute, the differences observed in Table 2 would appear to be the result of either the substituents in the molecular sieve or the framework structure. Comparison of H–[Ga]ZSM-5 to the H–ZSM-5 samples indicates that sites associated with Ga substitution are slightly weaker than those associated with Al, as other data have also suggested (13). For the aluminophosphates, the results indicate that the site strengths decrease as one goes from Mg^{+2} to Be^{+2} to Si^{+4}, with SAPO-5 having by far the weakest sites. Since the sites generated by Si substitution into the aluminosphosphate structure are due to the replacement of P, rather than Al as in the case of Mg and Be substitution, it is tempting to suggest that the four tetrahedral PO_4 groups surrounding the acid sites in MgAPO-5 and BeAPO-5 provide a more acidic environment than the four AlO_4 groups surrounding the sites in SAPO-5.

From the data in Table 2, it is evident that, with the exception of HY, the range of carbonyl ^{13}C chemical shifts for the silica–alumina molecular sieves is remarkably small, despite the fact that the framework structures are very different, particularly with respect to framework bond angles. These are important in determining the sizes of the cavities of the framework, and indeed, there is perhaps an inverse correlation with pore size, the largest shift being observed in H–ZSM-22 and the smallest in H–Y. However, it is unlikely that pore size alone can explain these observations.

This raises an interesting point. While all of the tetrahedral sites in a faujasite are equivalent, the same is not true for H–ZSM-5, which contains 12 inequivalent T sites. Based on the above arguments, one would expect the observation of a multiplicity of framework environments in H–ZSM-5 and thus a distribution of shifts associated with Al substitution at the 12 different tetrahedral positions. The fact that a single narrow line is observed in the MAS spectrum suggests that a single T site or lattice position is occupied (e.g., in the four-membered rings present at channel intersections (32, 33)), or more likely that the chemical shift is not sensitive to the differences.

In the case of acetone chemisorbed on H–ZSM-5, we have recently shown that the asymmetric lineshape, predominately determined by the shift anisotropy, is independent of concentration at room temperature for surface coverages less than one molecule per Brønsted site (9). From this and the absence of a temperature dependence of the isotropic shift in the present studies, it is reasonable to assume a high degree of molecular site localization at low surface coverages in all of the molecular sieves even at room temperature. However, the lineshapes and thus the anisotropies of the molecular motions of the adsorbed acetone molecules are not the same, but they correlate with the size of the channels. To a first approximation, the linewidth can be used as a rough measure of overall cavity dimensions, which in turn are related to the barriers and activation energies for molecular reorientation and translation.

With improved signal enhancement techniques and the availability of larger single crystals (34), more detailed information concerning the environment of the Brønsted-acid site, and perhaps even the location of this site in the zeolite framework, may be possible. We have recently begun a study to measure more precisely the elements of the chemical shift tensor of the ^{13}C carbonyl of acetone so that differences between the various zeolites can be characterized in terms of changes in electronic structure of the molecule. This should result in a more quantitative picture of the nature of the hydrogen bond. In addition, we are also examining the evolution of the chemical shift tensor as a function of both temperature and surface coverage for all of the zeolites in order to determine the mechanism for molecular reorientations (e.g., random diffusion or jumps) and also the barrier and activation energies for this dynamics for different framework structures. We believe the latter to be important in providing insights into the factors affecting rates of reactions, particularly bimolecular processes, that follow the initial chemisorption and rearrangements that occur at the Brønsted-acid sites.

CONCLUSIONS

(a) ^{13}C carbonyl chemical shifts of the probe molecule acetone, localized at a Brønsted-acid site in molecular sieves, provide a measure of the intrinsic site acidity and the molecular motion at the site.

(b) From the present data as well as the earlier surface coverage studies (9), localization, at least on the NMR time scale, can be achieved at surface coverages corresponding to less than one chemisorbed acetone molecule per Brønsted site, even at room temperature.

(c) From proton-decoupled, ^{13}C MAS spectra, the trace of the chemical shift tensor, which corresponds to the isotropic chemical shift, indicates that either a single framework T site can be identified as the acid site or more likely that differences in acidity of different T sites are relatively small.

(d) With few exceptions, the magnitude of the measured isotropic shifts for the large number of molecular sieves investigated falls into a very narrow range. By comparison with shifts observed in acid solutions of acetone, this range corresponds to an environment and thus, hydrogen

bonding comparable to that observed in a solution of trifluoroacetic acid.

(e) The room-temperature ^{13}C chemical shift lineshapes and linewidths provide a measure of the extent and nature of the anisotropic molecular motion of the chemisorbed acetone, which correlates with the size of the framework channel containing the Brønsted site.

ACKNOWLEDGMENT

This work was supported by NSF Grant CBT-8720266.

REFERENCES

1. Ward, J. W., *J. Catal.* **17,** 355 (1970).
2. Haag, W. O., and Dessau, R. M., *in* "Proceedings, 8th International Congress on Catalysis," p. 545. Verlag-Chemie, Weinheim, 1985.
3. Derouane, E. G., "NATO ASI Series," Series B, Vol. 221, p. 225 Plenum, New York, 1990.
4. Cardona-Martinez, N., and Dumesic, J. A., *Adv. Catal.* **38,** 149 (1992).
5. Kramer, G. M., McVicker, G. B., and Ziemiak, J. J., *J. Catal.* **92,** 355 (1985).
6. Chu, C. T. W., and Chang, C. D., *J. Phys. Chem.* **89,** 1569 (1985); Batamack, P., Doremieux-Morin, C., Vincent, R., and Fraissard, J., *J. Phys. Chem.* **97,** 9779 (1993); Freude, D., Hunger, M., and Pfeifer, H., *Z. Phys. Chem. N. F.* **152,** 171 (1987).
7. Karge, H. G., *in* "Catalysis and Adsorption by Zeolites" (G. Öhlmann *et al.*, Eds.), p. 133. Elsevier, Amsterdam, 1991.
8. Maciel, G. E., and Natterstad, J. J., *J. Chem. Phys.* **42,** 2752 (1965).
9. Biaglow, A. I., Gorte, R. J., and White, D., *J. Phys. Chem.* **97,** 7135 (1993); "Proceedings, Blue Hen NMR Conference, Wilmington, DE," June 1993.
10. Spiess, H. W., "NMR Basic Principles," Vol. 15, p. 55. Springer, Berlin, 1978.
11. Parrillo, D. J., and Gorte, R. J., *J. Phys. Chem.* **97,** 8786 (1993).
12. Ernst, S., Kokotailo, G. T., Kumar, R., and Weitkamp, J., *in* "Proceedings, 9th International Congress on Catalysis" (M. J. Philips and M. Ternan, Eds.), pp. 388–395. Chemical Institute of Canada, Ottawa, Canada, 1988.
13. Kofke, T. J. G., Kokotailo, G. T., and Gorte, R. J., *Appl. Catal.* **54,** 177 (1989).
14. Biaglow, A. I., Adamo, A. T., Kokotailo, G. T., and Gorte, R. J., *J. Catal.* **131,** 252 (1991).
15. Parrillo, D. J., Pereira, C., Kokotailo, G. T., and Gorte, R. J., *J. Catal.* **138,** 377 (1992).
16. Beyerlein, R. A., McVicker, G. B., Yacullo, L. N., and Zemiak, J. J., *J. Phys. Chem.* **92,** 1967 (1988).
17. Biaglow, A. I., Parrillo, D. J., Kokotailo, G. T., and Gorte, R. J., *J. Catal.* **148,** 779 (1994).
18. Kofke, T. J. G., Gorte, R. J., and Farneth, W. E., *J. Catal.* **114,** 34 (1988).
19. Kofke, T. J. G., Gorte, R. J., Kokotailo, G. T., and Farneth, W. E., *J. Catal.* **115,** 265 (1989).
20. Biaglow, A., Parrillo, D. J., and Gorte, R. J., *J. Catal.* **144,** 193 (1993).
21. Pereira, C., and Gorte, R. J., *Appl. Catal. A* **90,** 145 (1993).
22. Biaglow, A. I., Gorte, R. J., and White, D., *JCS Chem. Comm.* 1164 (1993).
23. K. R. Carduner, M. Villa, D. White, *Rev. Sci. Instrum.* **55,** 68 (1984).
24. Suwelack, D., Rothwell, W. P., and Waugh, J. S., *J. Chem. Phys.* **73,** 2559 (1980).
25. Biaglow, A. I., Gorte, R. J., and White, D., submitted for publication.
26. Abragam, A., "Principles of Nuclear Magnetism," Oxford Science, Oxford, 1961.
27. See Ref. (9), Fig. 4, p. 169.
28. See, e.g., R. G. Griffin, A. Pines, S. Pausak, and J. S. Waugh, *J. Chem. Phys.* **63,** 1267 (1965).
29. Kasab, E., Allavena, M., Evleth, E. M., Geissner, C., and White, D., unpublished results.
30. Parrillo, D. J., Gorte, R. J., and Farneth, W. E., *JACS* **115,** 12441 (1993).
31. Parrillo, D. J., Adamo, A. T., Kokotailo, G. T., and Gorte, R. J., *Appl. Catal.* **67,** 107 (1990).
32. Nicholas, J. B., Winans, R. E., Harrison, R. J., Iton, L. E., Curtiss, L. A., and Hopfinger, A. J., *J. Phys. Chem.* **96,** 10247 (1992).
33. Jacobs, P. A., and Martens, J. A., *Stud. Surf. Sci. Catal.* **33,** 321 (1987).
34. Schüth, F., and Althoff, R., *J. Catal.* **143,** 388 (1993).
35. Dolejsek, Z., Novakova, J., Bosacek, V., and Kublekova, L., *Zeolites,* **11,** 244 (1991).